

Geologic mapping of the Chaac-Camaxtli region of Io from Galileo imaging data

David A. Williams,¹ Jani Radebaugh,² Laszlo P. Keszthelyi,² Alfred S. McEwen,² Rosaly M. C. Lopes,³ Sylvain Douté,³ and Ronald Greeley¹

Received 13 November 2001; revised 22 April 2002; accepted 5 June 2002; published 26 September 2002.

[1] We produced a geologic/geomorphologic map of the Chaac-Camaxtli region of Io's leading anti-Jovian hemisphere using regional resolution (186 m/pixel) Galileo imaging data collected during orbit I27 (February 2000) integrated with lower resolution (1.4 km/pixel) color data, along with other Galileo imaging and spectral data. This is the first regional map of Io made from Galileo data. Nine color and geomorphologic units have been mapped, and the close proximity of dark and various colored bright materials suggests that there is an intimate interaction between (presumably) silicate magmas and sulfur-bearing volatile materials that produced a variety of explosive and effusive deposits in the recent geologic past. This region of Io is dominated by 11 volcanic centers, most of which are paterae that are analogous in morphology to terrestrial calderas but larger in size. Mapping of structural features indicates that most of the active regions occur in topographic lows, and less active or inactive paterae are associated with topographic highs. This indicates that crustal thickness variations influence magma access to the surface. Surface changes in this region since the Voyager flybys (1979) are relatively minor (additional bright and dark flows, color changes), although several active vents have migrated within paterae. This observation, along with the identification of the relatively regular spacing of paterae (~100–150 km) along a line, may indicate there are multiple interlacing fractures in the crust that serve as magma conduits from the interior. This connection between volcanism and tectonism may have implications for tidal heating mechanisms and their effect on Io's lithosphere. Some inactive patera floors may be evolving into bright plains material, which, if composed of silicates, might explain the strength of Io's crust to support steep patera walls and tall mountains. *INDEX TERMS:* 8450 Volcanology: Planetary volcanism (5480); 6218 Planetology: Solar System Objects: Jovian satellites; 5464 Planetology: Solid Surface Planets: Remote sensing; 5470 Planetology: Solid Surface Planets: Surface materials and properties; *KEYWORDS:* Io, geologic mapping, lava flows, paterae, planetary volcanism, Galileo mission

Citation: Williams, D. A., J. Radebaugh, L. P. Keszthelyi, A. S. McEwen, R. M. C. Lopes, S. Douté, and R. Greeley, Geologic mapping of the Chaac-Camaxtli region of Io from Galileo imaging data, *J. Geophys. Res.*, 107(E9), 5068, doi:10.1029/2001JE001821, 2002.

1. Introduction

[2] NASA's Galileo spacecraft has had a long and productive mission, acquiring data from at least 17 planetary objects in our solar system. Several flybys of each of Galileo's extended missions (Galileo Europa Mission (GEM): 1997–1999; Galileo Millennium Mission (GMM): 2000–2003) have been dedicated to obtaining data from Io, Jupiter's volcanically hyperactive innermost large moon. Galileo data are revolutionizing our understanding of Ionian

volcanism and tectonics. Perhaps the most important new finding was the discovery of very hot lavas, perhaps from active ultramafic eruptions (i.e., high-temperature, magnesium-rich silicate materials [McEwen *et al.*, 1998a; Geissler *et al.*, 1999; Davies *et al.*, 2001; Williams *et al.*, 2001a; Lopes *et al.*, 2001]), previously thought to have last erupted in the solar system on the ancient Earth.

[3] These latest discoveries about Io's volcanism based on Galileo data have been summarized by McEwen *et al.* [1998a, 1998b, 2000], Lopes-Gautier *et al.* [1999, 2000], Lopes *et al.* [2001], and Keszthelyi *et al.* [2001]. The last paper also described the Io data set obtained by the Solid State Imaging (SSI) experiment during Galileo orbits I24–I27 (October 1999 – February 2000). In this paper we focus on one of those observations, CAMAXT01 from orbit I27. This observation is a 12-frame, regional resolution (186 m/pixel) mosaic over the Chaac-Camaxtli region of Io's leading anti-Jovian hemisphere. We use analyses of this image mosaic (combined with lower resolution SSI color

¹Department of Geological Sciences, Arizona State University, Tempe, Arizona, USA.

²Lunar and Planetary Laboratory, University of Arizona, Tucson, Arizona, USA.

³NASA Jet Propulsion Laboratory, Pasadena, California, USA.

data), along with Near Infrared Mapping Spectrometer (NIMS) multispectral data, which provide temperature estimates and compositional information, to produce a geologic map of this region. From this map and these Galileo data, we infer the history of volcanic activity in this region, and discuss the broader implications for Io.

2. Background

2.1. Geologic Mapping of Io

[4] Geologic maps delineate the extent of different rock types and geologic structures on a planetary surface. However, in planetary science, we rarely have the ability to identify specific rock types. Instead, we use differences in geomorphology and color or albedo to infer different lithologies. While we use the term “geologic map” throughout this paper, strictly speaking these are geomorphologic maps. Nevertheless, geologic mapping from planetary images has enabled the interpretation of the geologic processes responsible for the evolution of planetary surfaces on several bodies in our solar system (e.g., Moon [Wilhelms and McCauley, 1971; Carr et al., 1971]; Mars [Scott and Carr, 1978; Greeley and Guest, 1987; Lucchitta, 1999]; Venus [Tanaka et al., 1994; Johnson et al., 1999; McGill, 2000]; outer satellites [Wagner et al., 1995; Bender et al., 1997]). A series of global, regional, and local geologic maps were produced from the Voyager images of Io obtained during the 1979 flybys [Moore, 1987; Greeley et al., 1988; Schaber et al., 1989; Whitford-Stark et al., 1991; Crown et al., 1992]. These maps were used to identify the range of volcano morphologies (e.g., shield volcanoes, pit craters, calderas, cones) and eruption products (e.g., lava flows, pyroclastic blankets) on Io, to interpret the colors of volcanic features relative to possible magma compositions, and to infer the sequence of volcanic eruptions in specific regions. These various maps showed that the surface of Io is dominated by complex, interfingered volcanic deposits from dozens of regionally active volcanoes, and that in specific regions it is possible to use planetary mapping to constrain the roles of various effusive vs. explosive eruptions, the relative importance of sulfurous vs. silicate compositions, and the relationships between tectonic and volcanic processes. However, with the return of new Galileo images and other data from Io, additional fundamental questions have arisen that might be addressed by new geologic mapping, including:

- What are the various roles of sulfur, mafic silicate, and ultramafic silicate volcanism in modifying Io’s surface, and how are they related?
- How important are SO₂ and other volatiles in influencing the style of eruptions on Io?
- Are there differences in volcanic vent morphologies, eruption styles, or eruption products between different volcanoes, regions or hemispheres?

[5] Our approach in this first geologic mapping project is to consider some of these questions while studying new Galileo data in a previously unmapped region of Io’s anti-Jovian hemisphere, which was poorly observed by the Voyager spacecraft. We will follow the established techniques for planetary mapping [e.g., Shoemaker and Hackman, 1962; Wilhelms, 1972, 1990; Tanaka et al., 1994], in order to identify the variety and sequence of volcanic materials in this region and how they have modified the surface.

2.2. Imaging of the Chaac-Camaxtli Region

[6] The Chaac-Camaxtli region is located in the leading quadrant of Io’s anti-Jovian hemisphere, and is defined as the region roughly bounded by Chaac Patera to the west and Camaxtli Patera to the east, between ~8–18°N and 160–130°W. This region of Io was poorly observed by the Voyager spacecraft, with image resolutions between 5–20 km/pixel [Smith et al., 1979a, 1979b] (Figure 1a). No geological studies of this region were done using Voyager data, except for mapping of the dark spots associated with Chaac Patera, Camaxtli Patera, and the ambiguous dark spot between them (now called Sobo Fluctus) as “Patera Floor Material” in the global geologic map of Crown et al. [1992]. Lower-resolution Galileo data show that the eastern paterae around Camaxtli Patera became more active (i.e., warmer hot spots) after Galileo orbit E15 (May 1998).

[7] The primary image product used for our mapping is the 12-frame mosaic of the Chaac-Camaxtli region (observation I27ISCAMAXT01, 186 m/pixel) obtained during the Galileo I27 flyby (February 2000), merged with the C21 low-resolution (1.4 km/pixel) color data (Figure 1b). The I27 encounter also included several very high resolution (5–10 m/pixel) images of the eastern caldera margin and floor of Chaac Patera (Figure 2) [McEwen et al., 2000; Keszthelyi et al., 2001]. These data were also used to help define and interpret the geologic units in this region. A series of names has been selected for the volcanic source regions (paterae and flucti) in the Chaac-Camaxtli region, which have received provisional approval from the IAU (Table 1, Figure 3). Henceforth, we will use these names when referring to specific volcanic features in our map region.

2.3. Color Interpretation on Io

[8] Interpretation of the colors of Io’s surface materials has been a contentious issue going back to the Voyager era [see, e.g., Sagan, 1979; Young, 1984]. A recent, thorough summary of previous and current spectral and compositional data on volcanogenic sulfur on Earth and Io was presented by Kargel et al. [1999], and a recent analysis of Galileo color data of Io was presented by Geissler et al. [1999]. Using multispectral analysis of Galileo global color data for Io at 413 nanometers (nm) (violet), 560 nm (green), 665 nm (red), and 757 nm (near-infrared), along with partial coverage over limited regions at 888 nm and 991 nm, and using available data from the NIMS, Geissler et al. [1999] defined four primary color units on Io: red materials, yellow materials, white materials, and dark materials. The red materials were subdivided into two subunits: regional red-orange units typically found in polar regions, and local red ring materials found around some volcanic hot spots like Pele [Geissler et al., 1999]. The yellow materials were likewise subdivided into two subunits: regional yellow materials covering large equatorial plains regions, and local greenish-yellow patches observed near or in some paterae. By comparing Galileo 4–6 point spectra with laboratory spectra of >650 rocks and minerals, Geissler et al. [1999] interpreted Io’s color units as being composed of the following materials: 1) Red units might be short-chain sulfur molecules (S₃, S₄), resulting from (in the case of the polar units) breakdown of cyclo-S₈ by charged particle irradiation [Johnson, 1997]), and (in the case of the red rings around Pele and other vents) by condensation from S₂-

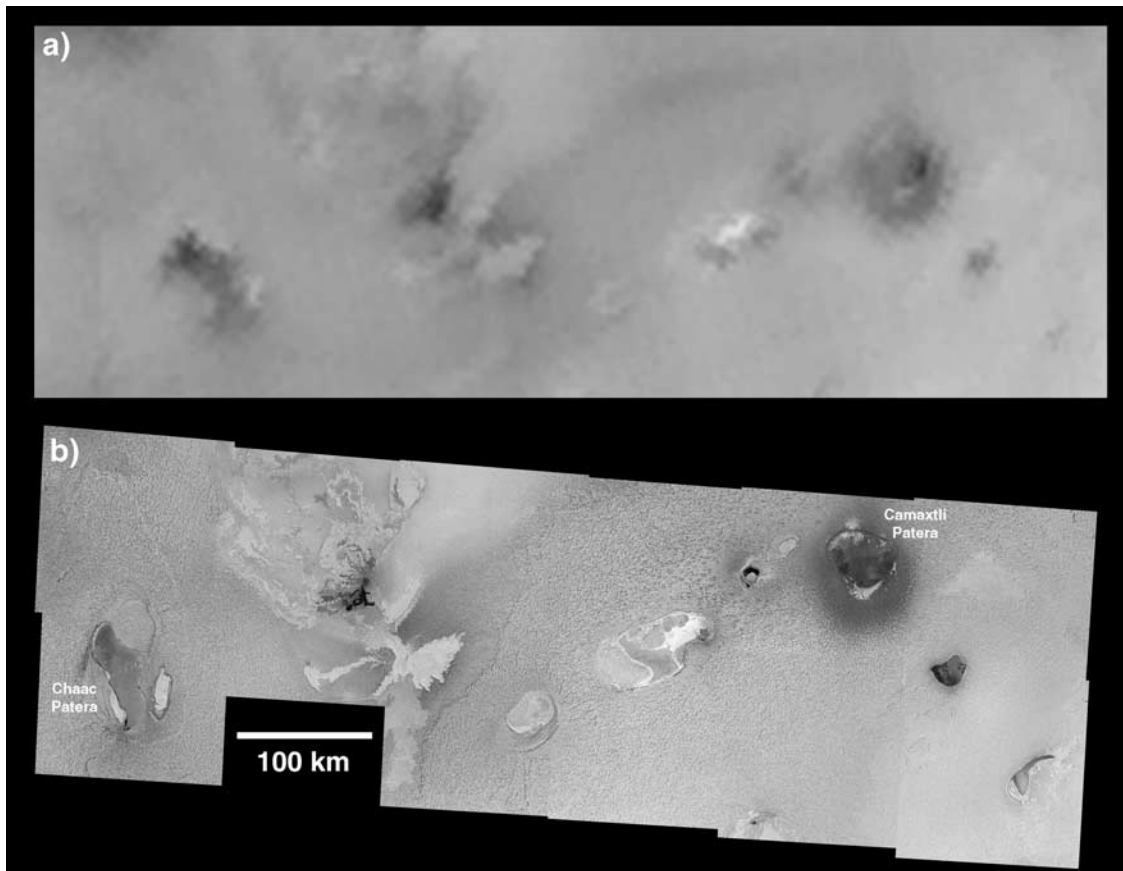


Figure 1. a) Best Voyager coverage of the Chaac-Camaxtli region, between 5–20 km/pixel. Extracted from NASA Planetary Photojournal Catalog Image #PIA00319. b) Galileo color mosaic of the Chaac-Camaxtli region. This image combines the 12-frame regional mosaic I271SCAMAXT01 (186 m/pixel) with a lower-resolution color mosaic C211SCOLOR01 (1.4 km/pixel). The I27 mosaic is an orthographic projection, centered on the sub-spacecraft point (1.8°N, 121.7°W), and was obtained at high phase angle, with illumination coming from the west. Non-horizontal faces are illuminated, enabling detection of scarps and depressions. From NASA Planetary Photojournal Catalog Image #PIA02566.

rich volcanic gases in their plumes [Spencer *et al.*, 2000]; 2) Yellow units might be cyclo-S₈ with or without a covering of SO₂ frosts deposited by plumes. Alternatively, Hapke [1989] showed that yellow color on Io can be produced by polysulfur oxide and S₂O without requiring large quantities of elemental sulfur; 3) Greenish-yellow patches might be either some sulfur compound contaminated by iron, or silicates such as olivine or pyroxene with or without sulfur-bearing contaminants; 4) White units are coarse- to moderate-grained SO₂ as indicated by NIMS [Carlson *et al.*, 1997; Douté *et al.*, 2001]; and 5) Dark spots, which mostly correlate with active hot spots [Lopes-Gautier *et al.*, 1999; Lopes *et al.*, 2001], are silicate lavas dominated by Mg-rich orthopyroxene (enstatite or bronzitelypersthene), as indicated by the strong 0.9 μm absorption [Geissler *et al.*, 1999].

[9] The colors of sulfurous materials on Io change as they age. By aging, we refer to irradiation of surface materials, which tends to alter the color of sulfur materials (e.g., cyclo-S₈ develops metastable impurities S₃ and S₄, with colors ranging from brownish-yellow to grayish-yellow to orange: [Nash and Fanale, 1977; Nelson and Hapke, 1978; Steudel *et al.*, 1986; Hapke and Graham, 1989; Nelson *et al.*, 1990].

Red materials tend to fade over a period of months. For example, red material on the floor of Pillan Patera changed to a greenish color [Phillips, 2000; Keszthelyi *et al.*, 2001]. The interpretation of this color change at Pillan is that the short-chain sulfur (S₃, S₄) changes with time to S₈ if it lands on cool plains material, but turns green if it lands on warm lava and interacts with it [Phillips, 2000]. Dark materials tend to brighten with time, as they develop coatings of sulfurous materials from plume deposits [Nash *et al.*, 1986]. Bright materials tend to darken over time, as they interact with underlying and superposed materials. Kargel *et al.* [1999] has reviewed the effects of these processes on sulfurous materials, and indicates that these color changes occur on timescales that are geologically important for Io (days to years). We think this may be of some importance in helping to determine relative ages. For example, where we can map superposed bright flows in Sobo, the older flows are somewhat darker.

2.4. Galileo NIMS Data of the Chaac-Camaxtli Region

[10] Galileo's NIMS instrument obtained wavelength coverage (1.0–4.7 μm) over parts of the Chaac-Camaxtli region during each of the flybys I24–I27 (Figure 4).

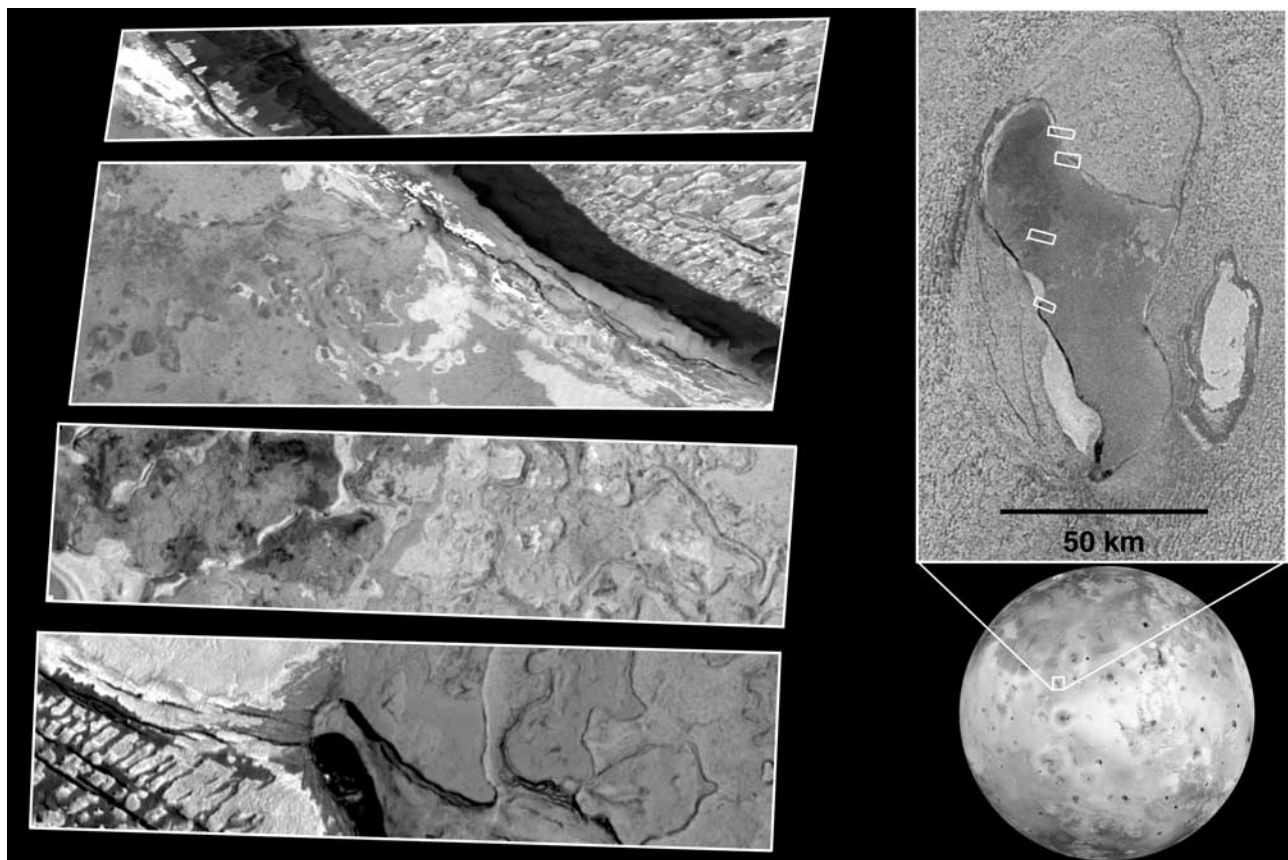


Figure 2. High-resolution (7–8 m/pixel) Galileo solid-state imaging (SSI) data of four areas in and around Chaac Patera from orbit I27 (February 2000). The morphology of materials on the floor of Chaac has been interpreted by *McEwen et al.* [2000] and *Keszthelyi et al.* [2001] (based on comparison to aerial photographs and field studies of Hawaiian lava flow features) as similar to volcanic materials found on Hawaiian compound pahoehoe inflationary flow fields, indicating effusive lava flow emplacement.

Table 1. Proposed Names for Newly Identified Volcanic Features in the Chaac-Camaxtli Region^a

Name	Lat (N)	Lon (W)	Size, km	Hot Spot	Notes	Origin of Name
Chaac Patera	11.8	157.2	92.7	Y	Seen by NIMS, orbits I25 and I27	Mayan god of thunder and rain
Balder Patera ^b	11.3	155.8	43.7	N		Norse god of light
Sobo Fluctus ^b	14.0	150.0	N/a	Y	Seen by NIMS, orbits I24 and I27	Voodoo spirit of thunder
Grannos Patera ^b	10.9	145.0	42.8	N		Gaulish sun god
Ababinili Patera ^b	12.6	141.8	103.2	N		Chicksaw fire and sun god
Ruaumoko Patera ^b	14.5	139.3	18.5	Y	Seen by NIMS, orbits I24 and I27	Polynesian god who causes earthquakes and volcanoes
Steropes Patera ^b	15.6	138.8	N/a	N		A Greek cyclops, created thunderbolts for Zeus
Camaxtli Patera	15.0	136.4	56.3	Y	Seen by NIMS/SSI, orbits E15, I24, I27	Aztec god of thunder, tornado, and war
Tien Mu Patera ^b	12.0	133.9	27.3	Y	Seen by NIMS, orbits I24 and I27	Chinese mother-lightening
Utu Patera ^b	9.4	132.0	35.2	Y	Seen by NIMS, orbits I25 and I27	Sumerian sun god
Mentu Patera ^b	6.7	139.0	98.3	Y	Seen by NIMS, orbit I27	Egyptian god of the rising sun

^a Refer to Figure 3.

^b Provisional name.

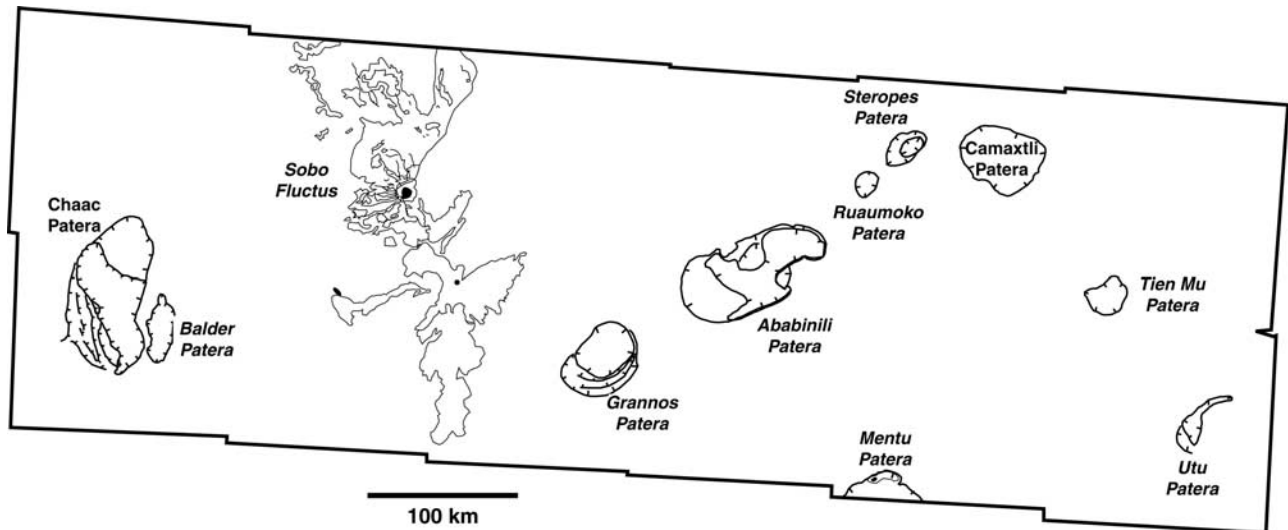


Figure 3. Diagram of the Chaac-Camaxtli region, with provisional (*italics*) names of newly identified volcanic features.

Processing of the NIMS data enabled identification of volcanic hot spots, from which temperature estimates were made [Lopes *et al.*, 2001]. As Figure 4 shows, there are multiple hot spots in the Chaac-Camaxtli region, corresponding to dark material (mostly confined in paterae) interpreted to indicate recent volcanic activity [see Lopes *et al.*, 2001, Table 4]. As reported by Lopes *et al.* [2001], the temperature estimates of the hot spots in this region are thought to represent cooling silicate lavas.

[11] Further processing of NIMS data has been done to quantify the nature of sulfur dioxide (SO₂) frost on Io's surface [Douté *et al.*, 2001]. Specifically, Douté *et al.* [2001] used NIMS data to create maps of both SO₂ frost abundance and physical character (*i.e.*, grain size) from studies of backscattering behavior and spectral modeling. Several NIMS mosaics cover portions of the Chaac-Camaxtli region at various resolutions, in which the most useful data for this study is shown in Figure 5. NIMS observation I27INMOSAIC01 covers parts of Chaac Patera and Balder Patera (the smaller elongate patera to the southeast of Chaac). The floor of Balder Patera contains a bright whitish material, which has a high abundance of SO₂ (~70–90%). This white material has been interpreted as a 'lake' of frozen SO₂ ice, perhaps effusively emplaced [Smythe *et al.*, 2000]. However, this hypothesis has not yet been critically studied.

2.5. Surface Ages

[12] Io is the only rocky body in the solar system that is devoid of impact craters. This fact is likely attributable to the rapid covering of impact craters by materials emplaced from Io's many active volcanoes [Smith *et al.*, 1979a]. Recent estimates of cratering rates on the Galilean satellites suggest that a 20-km diameter crater should form on Io every 2.3 Ma [Zahnle *et al.*, 1999]. Thus, the absence of large craters everywhere suggests that the surface of Io is less than a few tens of million years old [McEwen *et al.*, 2000], perhaps as young as a few million years old. Structural features in the crust, such as paterae, mountains, or linear tectonic trends may be older than a few tens of

millions of years, but absolute ages cannot be determined without samples for radiometric dating or impact craters for various crater statistical methods [*e.g.*, Boyce, 1976; Neukum and Ivanov, 1994]. Relative dating of surface features can be performed using: 1) superposition, 2) brightening of dark areas between Voyager and Galileo images, and 3) correlation of NIMS hot spots (presumably from recent activity) with surface features. These techniques are used in this study, and we assume that features in our map range in age from ~20 years (for the freshest flows seen in the Galileo mosaic but not visible in the Voyager images) to <<100 Ma.

3. Material Units

[13] Study of the Galileo I27 SSI mosaic of the Chaac-Camaxtli region enabled identification of features that were ambiguous in the lower resolution Voyager and early Galileo images. Generally, this region is dominated by textured bright plains and at least 11 separate volcanic centers, most of which appear to be paterae (*i.e.*, depressions, not of impact origin) that are reminiscent of terrestrial calderas with various degrees of tectonic modification. The paterae show a range of sizes and shapes, from a 15 km diameter circle (Ruumoko Patera) to a 105 km × 48 km ellipse (Chaac Patera). The non-circular shapes may indicate these paterae were formed, at least in part, due to interaction between volcanic and tectonic processes [Jaeger *et al.*, 2001; Radebaugh *et al.*, 2001]. In the case of Chaac Patera, shadow measurements on the high resolution images show that the patera wall is 2.7 km high with a 70 degree slope [Radebaugh *et al.*, 2001]. Most paterae appear to be at least partly filled by a variety of bright and dark materials [Keszthelyi *et al.*, 2001; Radebaugh *et al.*, 2001], in which spectral analysis of the dark materials suggests the presence of Mg-rich orthopyroxene, indicative of silicate volcanism [McEwen *et al.*, 1998a; Geissler *et al.*, 1999]. The bright plains in some areas are modified by structural features (*e.g.*, scarps), partly covered by effusive or explosive deposits from the paterae or Sobo Fluctus, or

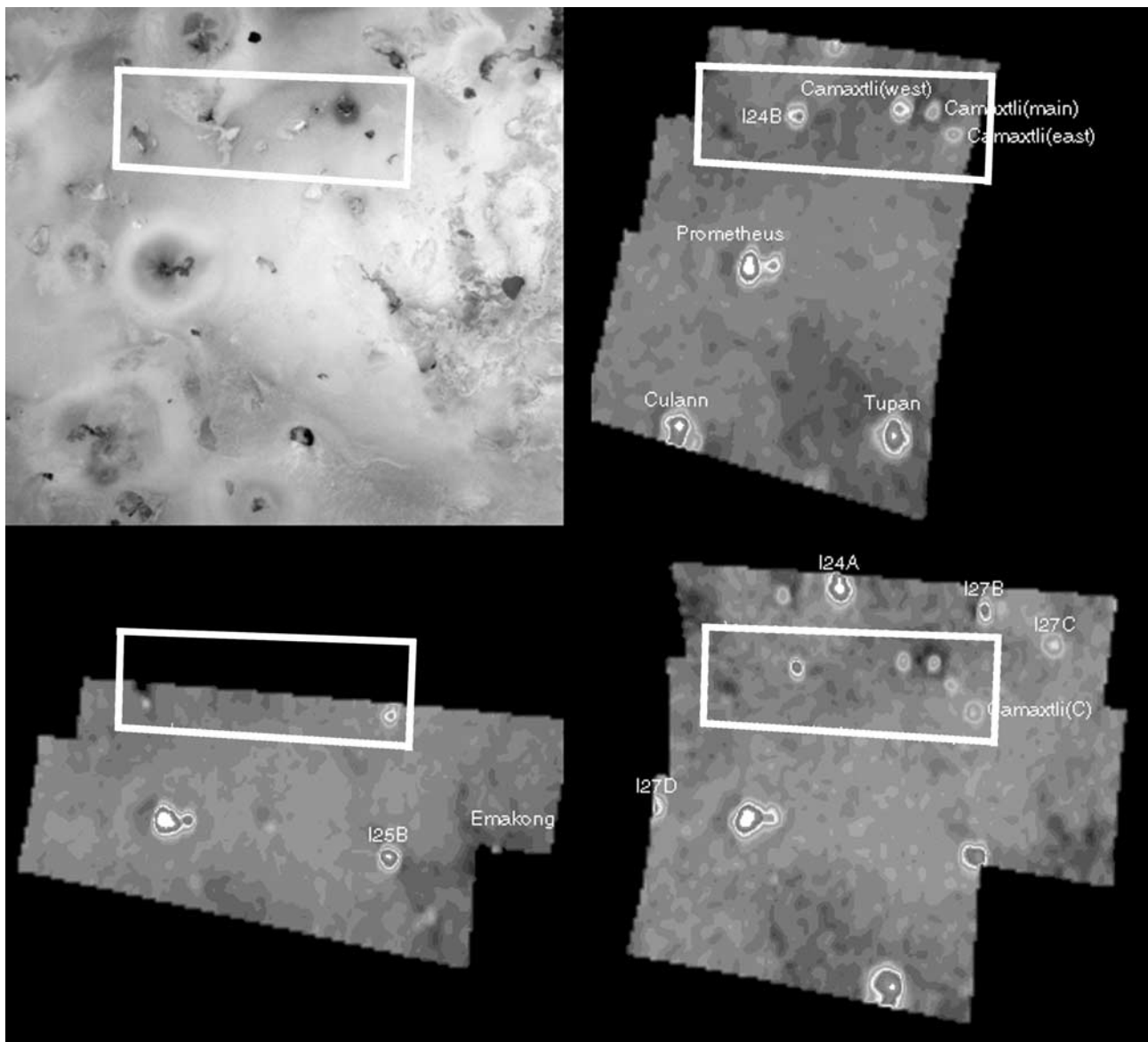


Figure 4. Galileo SSI (upper left) and Near Infrared Mapping Spectrometer (NIMS) data covering the Chaac-Camaxtli region (white box) from orbits I24 (upper right), I25 (lower left), and I27 (lower right). Bright spots indicate warm volcanic heat sources, several of which were detected in the Chaac-Camaxtli region [Lopes *et al.*, 2001]. The hot spot labeled I24B is Sobo Fluctus, Camaxtli (west) is Ruaumoko Patera, Camaxtli (main) is Camaxtli Patera, Camaxtli (east) is Tien Mu Patera, and Camaxtli (C) is Utu Patera.

contain unusual regions of different texture (the primary feature of this type is in the uppermost right frame, and may be an extinct, partly buried patera with an irregular margin).

[14] Our analysis of the Galileo images of the Chaac-Camaxtli region suggests that there are at least 9 distinct morphologic units that can be identified. In all cases relative albedos and colors are used, along with morphological differences, to define material units. Type localities of each material unit are shown in Figure 6.

3.1. Hummocky Bright Plains Material, p_b

[15] Description: Hummocky surface with albedo intermediate between Dark and Bright Patera Floor materials. Color image shows some variation in the plains between

darker and brighter areas, perhaps related in part to variations in SO_2 grain size or abundance [Douté *et al.*, 2001]. Plains near some volcanic centers are mantled by either bright or dark diffuse materials. Hummocks do not appear to follow a clear pattern at medium resolution, but at high resolution near the eastern margin of Chaac Patera (Figure 2) the hummocks can be seen to be bright, irregular mounds in a matrix of darker, smoother material. The mounds are oriented roughly perpendicular to the patera margin (i.e., radial to the patera). Interpretation: Modified explosive and effusive volcanic deposits. The source of the hummocky texture is a mystery, but ideas include: a) rhythmic features produced by SO_2 sublimation, b) dunes deposited by pyroclastic activity [McEwen *et al.*, 2000], c) tectonic modification of crustal materials

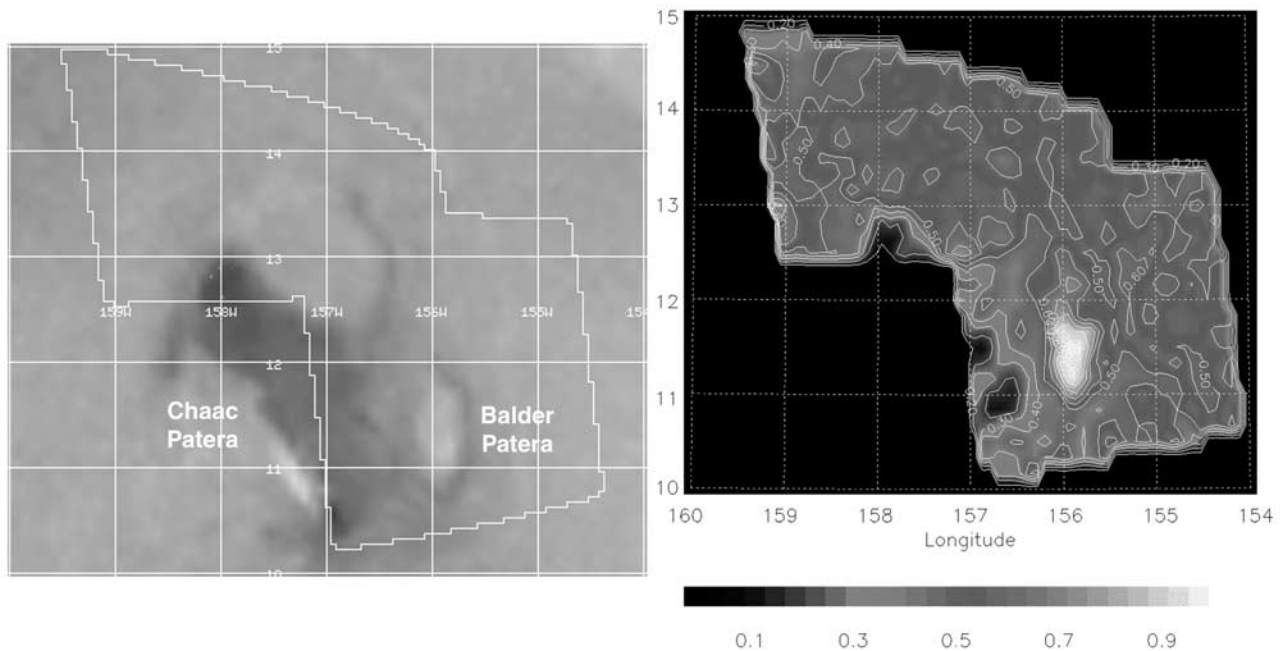


Figure 5. (Left) Low-resolution (1.4 km/pixel) Galileo image covering Chaac and Balder Paterae from orbit C21. White boundary marks the coverage of I27 NIMS observation. (Right) NIMS SO₂ abundance map covering part of Chaac Patera and Balder Patera, after *Douté et al.* [2001]. Balder Patera, southeast of Chaac, has a high abundance of SO₂ frost, which has been suggested to have been emplaced effusively [*Smythe et al.*, 2000].

[*Moore et al.*, 2000], d) gravitational slumping [e.g., *Moore et al.*, 2001], e) tidal flexing, or other presently unknown processes. We consider the nature of the bright plains further in section 5.

3.2. Dark Patera Floor Material, pf_d

[16] Description: Green to gray to black surface with considerable variation in albedo and texture. Appears smooth at low to medium resolution, but at high resolution in Chaac Patera (Figure 2) appears to be an interwoven mixture of bright and dark features, irregular hummocks, and pits. NIMS data suggest that little sulfur dioxide is present (Figure 5) [*Lopes et al.*, 2001]. Interpretation: Overall, the morphology of the floor of Chaac Patera shows a striking resemblance to the surface of the Kilauea caldera floor [*Keszthelyi et al.*, 2001]. Dark patera floors form by flow of low-viscosity, dark, mafic to ultramafic lavas. Some bright materials may be due to sulfurous lavas, or to silicate interaction with and/or contamination by sulfur- and/or iron-rich materials from plume deposits. Based on comparisons to aerial photographs of well-studied Hawaiian flow features, some hummocks and pits appear to be inflation features while other pits appear to be vent conduits.

3.3. Bright Patera Floor Material, pf_b

[17] Description: Bright white to orange to light gray unit with smooth surface at high and medium resolution. Has distinct contact with surrounding terrain, usually found within paterae but can also occur on their rims. Galileo NIMS data indicate a high abundance of sulfur dioxide in

Balder Patera (Figure 5). Interpretation: White material may be frozen layers of relatively pure sulfur dioxide (SO₂) ice or snow; orange to gray material may be SO₂ or sulfur-rich ice or snow with other contaminants.

3.4. Bright Flow Material, f_b

[18] Description: At medium resolution, appears as smooth bright (orange to yellow to white) linear flows. Lengths are greater than widths, but less so than with the dark flows. In the Chaac-Camaxtli region, bright flows are generally more areally extensive than dark flows. Contacts are distinct with surrounding terrain. Range of albedos and crosscutting relations can be used to define age relationships in some cases to separate younger (f_{b2}) from older (f_{b1}) flows. Interpretation: Low-viscosity lava flows from effusions of sulfur-rich materials. Range of colors may represent either variation in lava composition or coating of sulfur or darker silicate flow surfaces by sulfurous pyroclastic materials or condensates. Some bright flows could represent sulfurous plains material that was melted and remobilized by adjacent silicate magmas or lavas [*Greeley et al.*, 1984]. Similarly, we think heat from dark flows at Prometheus has apparently caused sublimation of SO₂ at flow fronts, resulting in white plumes of redeposited SO₂ frosts radial to flow margins [*McEwen et al.*, 2000; *Milazzo et al.*, 2001].

3.5. Undivided Flow Material, f_u

[19] Description: Terrain consisting of interfingered bright and dark flows with a range of albedos. Contacts are not distinct and sometimes hard to distinguish, making it

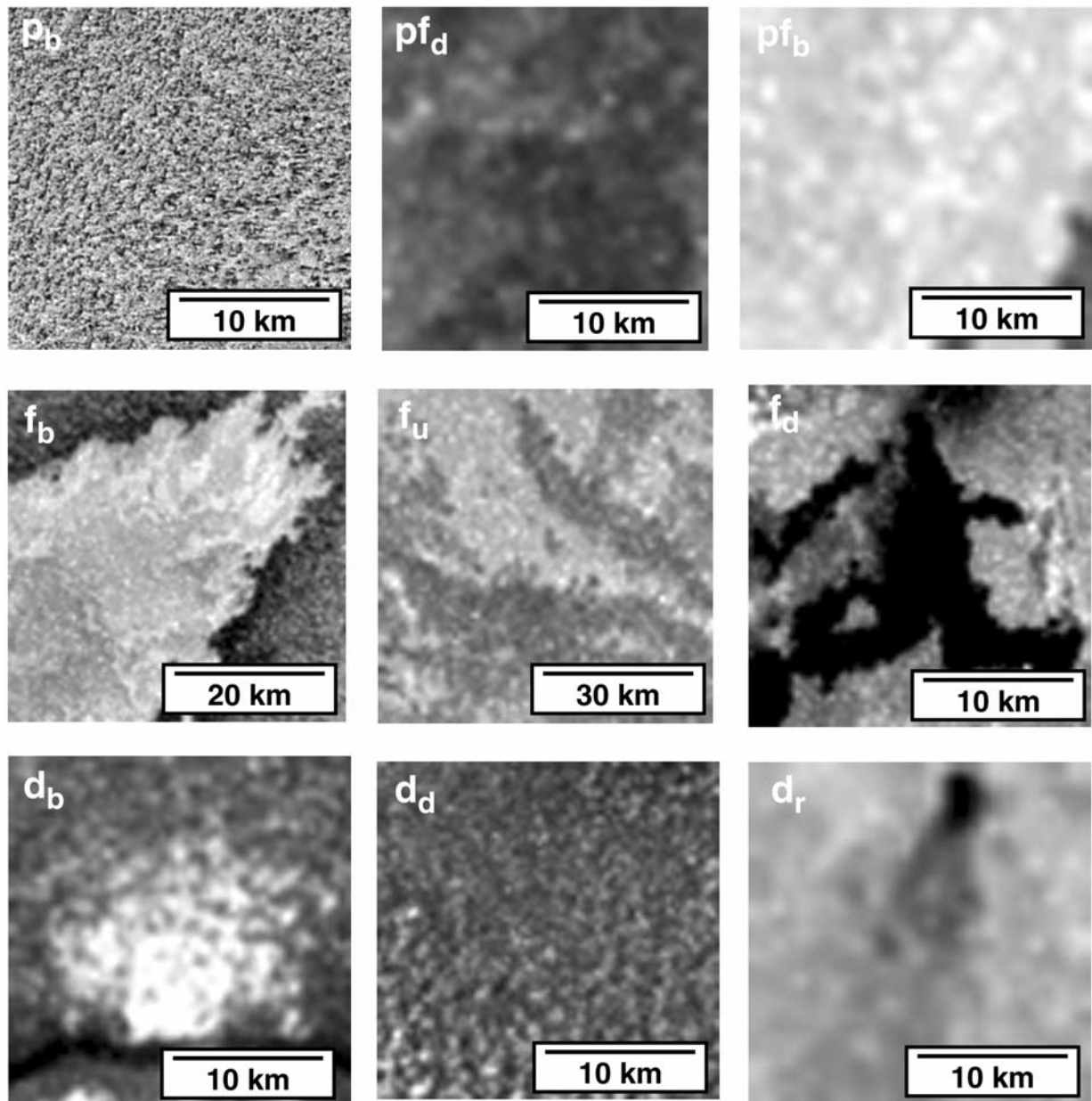


Figure 6. Type examples of geologic units in the mapped area. Bright plains material, p_b ; dark patera floor material, pf_d ; bright patera floor material, pf_b ; bright flow material, f_b ; undivided flow material, f_u ; dark flow material, f_d ; bright diffuse material, d_b ; dark diffuse material, d_d ; red diffuse material, d_r .

difficult to break out individual flows. Interpretation: Flows from various sulfur-rich and/or silicate-rich effusive eruptions, older than materials defined as f_b or f_d . Range of albedos due to coating of flow surfaces by pyroclastic materials or condensates, and/or the effects of aging in the Ionian environment.

3.6. Dark Flow Material, f_d

[20] Description: At medium resolution, appears as smooth dark (black to brown) lobate flows with lengths \gg widths. Contacts with surrounding terrain are sharp, and flows extend toward and into apparent topographic lows.

Range of albedos and crosscutting relations can be used to define age relationships in some cases to separate younger (f_{d2}) from older (f_{d1}) flows. High-temperature hot spots occur within dark flows as noted in NIMS observations (Figure 4). For example, in the case of Chaac Patera, the hot spot occurs in the dark material at the southern tip of the patera. Interpretation: Low-viscosity lava flows from mafic or ultramafic silicate eruptions [Murase and McBirney, 1973; Williams *et al.*, 2000]. Range of albedos in dark flows due to variation in lava composition, coating of flow surfaces by sulfurous pyroclastic materials or condensates, or other effects of aging in the Ionian environment (e.g.,

degradation of the flow surfaces by cosmic ray or charged particle bombardment.)

3.7. Bright Diffuse Material, d_b

[21] Description: Appears to thinly mantle underlying materials. Occurs in small patches near volcanic centers (d_{b2}) (e.g., Camaxtli Patera). More widespread (covering tens of kilometers, d_{b1}), thicker yellowish units also occur, burying plains units. Interpretation: Explosively emplaced sulfurous and/or sulfur dioxide pyroclastic deposits. Volatiles may be remobilized crustal material [Kieffer *et al.*, 2000; Milazzo *et al.*, 2001].

3.8. Dark Diffuse Material, d_a

[22] Description: Appears to thinly mantle underlying materials. Occurs either in patches near or as a halo around volcanic centers, decreasing in optical density with distance from volcanic centers (e.g., Camaxtli Patera). Interpretation: Explosively emplaced silicate and/or black sulfur pyroclastic deposits. Spectral analysis of the dark diffuse deposit from the 1997 Pillan eruption is consistent with Mg-rich silicates [Geissler *et al.*, 1999].

3.9. Red Diffuse Material, d_r

[23] Description: Usually highly transparent and transitory, thinly mantles units that occur around some highly active volcanic centers. Only one very small spot has been mapped, on a large bright flow in Sobo Fluctus. Interpretation: Explosively emplaced pyroclastic deposits or frozen magmatic gases, possibly colorized by unstable, short-chain sulfur polymers. The metastable S_3 and S_4 allotropes, red when quenched in their high-temperature forms [Spencer *et al.*, 1997], could act as colorizing contaminants within bright, transparent material such as SO_2 [Geissler *et al.*, 1999]. Source appears to be primary magmatic gas [Spencer *et al.*, 2000; Keszthelyi *et al.*, 2001].

4. Structures

[24] Unlike the Galilean satellites Europa and Ganymede, Io has fewer continuous structural features visible at regional resolution [cf. Schenk and McKinnon, 1989; Collins *et al.*, 1997]. This is likely due to the extensive volcanic resurfacing, in which pyroclastic deposits, plume deposits, and lava flows quickly cover up many surface features. However, using both the high-resolution I27 mosaic of the Chaac-Camaxtli region (taken at high sun angle), along with several low-resolution global images showing parts of the Chaac-Camaxtli region taken at low sun angle, it is possible to map lineaments, scarps, and other features in this region. Shadow lengths and directions reveal that all of the paterae have depressed interiors, similar to terrestrial calderas. Sobo Fluctus appears to occupy a topographic low, surrounded by small scarps rising up to higher plateaus. Several of the paterae seem to occupy local topographic highs, particularly Chaac and Grannos Paterae.

5. Discussion

[25] We have synthesized the data discussed above to produce a geologic map of the Chaac-Camaxtli region, based on the Galileo SSI mosaic I27ISCAMAXT01, including a stratigraphic correlation of the map units (Figure 7). In

each of the following sections we discuss specific aspects of the geology of the Chaac-Camaxtli region as inferred from our map and supporting data.

5.1. Changes Since Voyager

[26] Comparison of Voyager and Galileo images is perilous because Voyager's camera did not image Io beyond orange wavelengths, and Galileo color images of Io use 756 nm as our "red" component in RGB images. Also, there are variations in resolution and lighting conditions (e.g., contrast reversals can occur with differences in phase angle). Thus, it is difficult to make definitive statements about volcanically induced surface changes. However, using relative albedo instead of color, we have made the following observations of surface changes. First, there is no evidence of large-scale (100s km) surface changes in this region over the last 21 years. Second, ill-defined spots on the surface in Voyager images can now be resolved into specific surface features, namely paterae or flucti (lava flow fields). Third, a series of small-scale changes are apparent. Additional dark flows have been emplaced in Sobo Fluctus, and in Camaxtli, Ruaumoko, Tien Mu, and Utu Paterae. Ruaumoko, indistinct in the Voyager image, has developed into a resolvable patera with a dark lava lake containing an island of bright material, similar in morphology to Loki. Vent migration (from the east side of the patera to the west side) has apparently occurred in Camaxtli and Tien Mu, whereas in Utu the vent has migrated from the southwest to the northeast, and in Chaac the vent has migrated from the north to the south within the patera. The white deposits in Balder Patera may have expanded in areal extent since 1979. Additional bright flows have been emplaced in Sobo Fluctus, including a thin flow trending southwest to northeast from a small depression west of the main bright flow, and the large main bright flow has extended to the southwest. Apparent brightening has occurred in the floors of Chaac and Ababinili Paterae. Finally, with the possible exception of Ruaumoko Patera, no new large eruptive centers have formed in the 21 years between Voyager and Galileo observations.

5.2. Volcanic Features and Eruption Styles

[27] Based on the study of surface changes since Voyager, it appears that volcanic activity associated with migrating vent positions is the primary process responsible for changes in the paterae in this region. The styles of volcanic activity at individual centers have not changed with time, although different centers have different proportions of explosive vs. effusive volcanism. For example, there is an extensive aureole of dark pyroclastic material around Camaxtli, whereas there are only a few scattered small dark diffuse patches at Chaac. This, coupled with the observation that the quantity of dark patera floor material in Chaac is less than that in Camaxtli, possibly indicates a decline in activity in Chaac relative to Camaxtli. This is supported by NIMS data, which show a weaker hot spot at Chaac compared to Camaxtli. Bright yellowish (S-rich?) diffuse deposits are quite extensive in this region (Sobo is the likely source of the north-central deposit; the source of the southeastern deposit is unclear, but may come from vents in the northern part of Bosphorus Regio to the south of the map area). In contrast, white (SO_2 ?) diffuse deposits

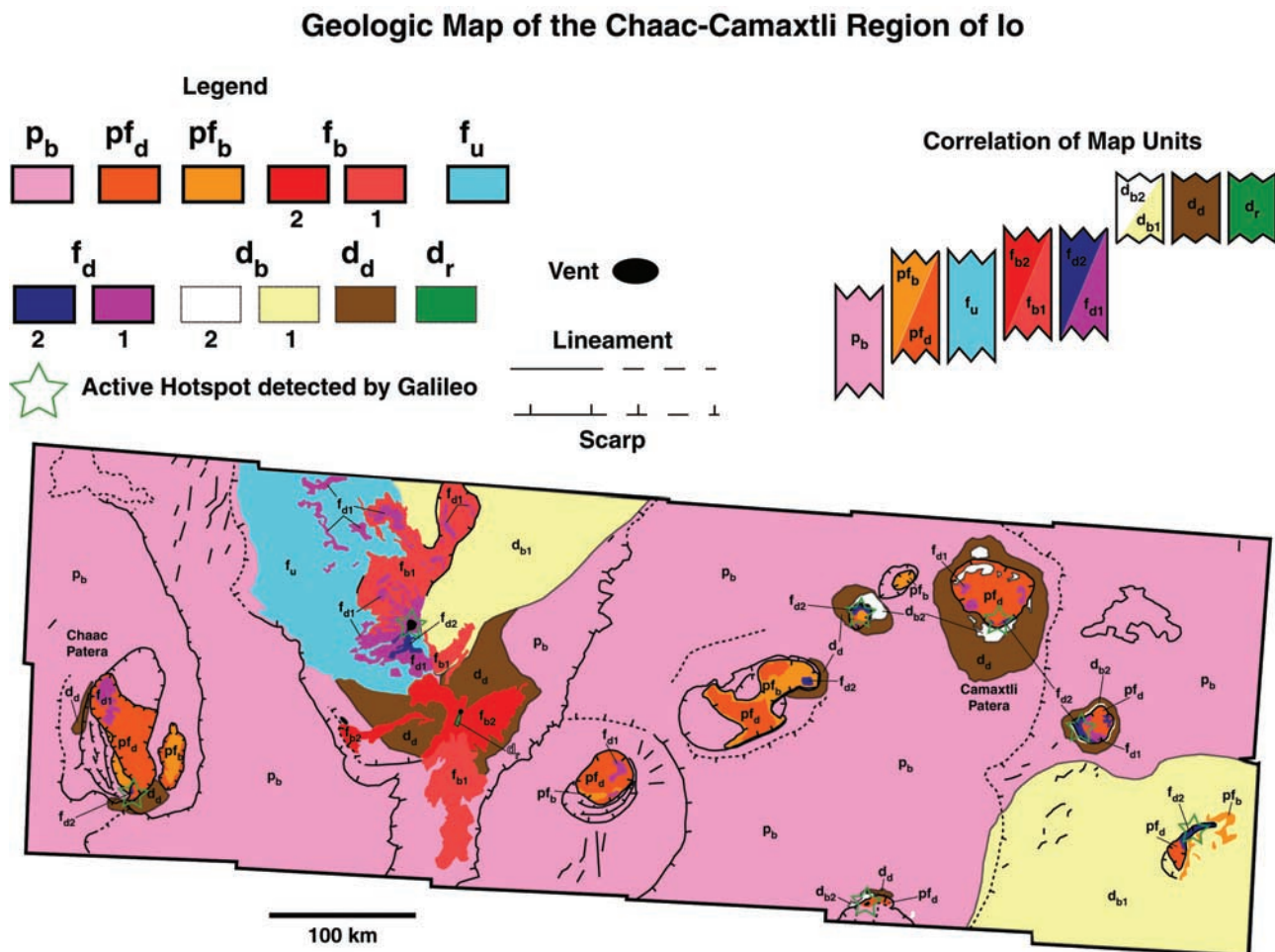


Figure 7. Geologic map of the Chaac-Camaxtli region, including a stratigraphic correlation of map units. Based on Figure 1b. Vent symbols refer to visible dark spots that appear to be the source of volcanic products (mostly in Sobo Fluctus). We assume most vents associated with active hot spots (green stars) inside paterae are buried by dark flow material, f_d . Dashed lines for lineaments and scarps are not as easily discerned in the image—they could be buried, or simply less well-exposed.

are limited to small patches around Ruaumoko, Camaxtli, and Mentu Paterae in our map area. These relatively small deposits differ in size from more extensive white diffuse deposits that occur radial to flow margins at the volcano Prometheus. These deposits are apparently white plumes of redeposited SO_2 frosts, produced when heat sublimates SO_2 in the plains at active lava flow fronts [McEwen *et al.*, 2000; Milazzo *et al.*, 2001].

[28] The presence of both bright and dark flows suggests that a range of lava compositions have been erupted onto the surface, including both silicate and possibly multiple sulfur-bearing compositions. This assumes that at least some of the bright flows in the Chaac-Camaxtli region are genetically sulfuriferous flows and not simply darker silicate flows that have been mantled by sulfuriferous pyroclastic materials. This assumption seems valid for at least the fresh bright flows left of center in Sobo Fluctus (Figure 7), which do not appear mantled but rather appear to be composed of a uniformly, inherently bright material. It would also be difficult to just coat a dark lava flow with bright material without also coating the surrounding units.

[29] White sulfur dioxide might be considered a subset of the sulfuriferous materials found in this region, based on color differences. For example, near the western scarp boundary in Sobo, southwest of the dark center, is a small depression that contains a white deposit that appears similar in color and texture to that in Balder Patera. A bright flow (mapped as fb_2) emanates from this white deposit, which is similar in color and morphology to the primary Sobo bright flows. NIMS indicates the white material in Balder Patera is almost pure SO_2 , which Smythe *et al.* [2000] think may have been emplaced as a flow. However, at our resolution we can see no morphological features indicative of flows within Balder. This small bright flow near the Sobo western scarp boundary could be a SO_2 flow rather than a sulfur flow. Another example of a possible SO_2 flow may occur in Ababinili Patera, in which a distinct zone of white material exists between the orange patera floor and the pink plains material. It might be possible that residual heat from the orange patera floor material mobilizes SO_2 in the plains, which then moves downhill into the caldera and may have begun to cover the orange patera floor. Alternatively, it is

possible that the orange and white materials are of similar compositions, but that they are of different temperatures.

[30] A fundamental question from the Voyager era is whether sulfur flows on Io are *primary* flows (i.e., resulting from sulfur magma eruptions), or whether sulfur flows are *secondary* flows, i.e., resulting from melting of sulfurous country materials by heating from nearby silicate lavas or magmas. This question is difficult to answer, even with the new Galileo SSI and NIMS data. *Greeley et al.* [1984] noted that a Mauna Loa sulfur flow appeared to result from remobilized fumarolic sulfur deposits, and suggested this process might occur on Io. From our mapping of the Sobo flows, we find both dark and bright flows that occur in close proximity, and that they have apparently erupted in close proximity over time. There is no variation in color, albedo, or morphology that indicates to us that one dark flow may have caused one bright flow. Rather, the close proximity of dark flows and bright flows in many areas on Io (e.g., Zamama in the I24 high resolution images) suggests to us that it is likely that hot silicate magmas can melt their sulfurous surroundings, resulting in sulfur-bearing flows adjacent to sources of dark silicate volcanism. We detect no changes in any of the bright flow morphologies that might indicate the rheological changes that are thought to occur between high-, intermediate-, and low-temperature sulfur flows [*Fink et al.*, 1983; *Pieri et al.*, 1984; *Williams et al.*, 2001b]. However, we cannot rule out primary sulfur flows.

5.3. Bright Plains Formation

[31] The genesis of Io's bright plains (and particularly, the formation of the hummocky texture observed near paterae margins) remains a mystery. One of the first ideas regarding the radial nature of the hummocks relative to the patera margins was that they might be depositional features from pyroclastic flow deposits [*McEwen et al.*, 2000]. However, this texture is found throughout Io's bright plains, and it seems unlikely that pyroclastic flows would be globally extensive. *Moore et al.* [2000] suggested (based on study of hummocky terrain in I24 images of Ot Mons) that the hummocks are ridges that are the manifestation of compressional folds in a weak layer of sulfur-rich material overlying a shallow decollement or a ductile sub-surface layer. These hummocks are regularly spaced and of a fairly uniform size (~1–2 km long, 250–500 m wide), but with large amphitheatres cut into them that are not apparent in the hummocky plains outside Chaac. With the limited data available, we think it is premature to exclude any hypothesis on the genesis of the hummocky texture. Gravity slumping or unusual sublimation/degradation effects [see *Moore et al.*, 2001] also remain possible explanations.

[32] The Chaac-Camaxtli region occupies a significant fraction of Io's equatorial bright plains. According to *Douté et al.* [2002], the SO₂ areal abundance for these plains is relatively uniform at a scale of 10 km, close to a background value of approximately 45%. This constant level is often associated with large grain sizes, 300 microns or more. *Douté et al.* [2002] show that correlating maps of SO₂ abundance and granularity derived from Galileo NIMS data provide insights about the physical state of SO₂ on Io. More precisely, four different SO₂ physical units can be distin-

guished that indicate zones of condensation, metamorphism and sublimation for SO₂ frost. The equatorial plains seem to achieve some kind of steady state between these three processes. Continual and long term condensation of the tenuous global atmosphere or of volcanic SO gases migrating from remote plumes may occur day or night, though with a low deposition rate. During the daytime, the condensed frost undergoes slow metamorphism under sunlight and may even sublimate at some locations. As a consequence, SO₂ "frost," which is evolved and moderately abundant, likely undergoes numerous cycles of sublimation/condensation at low latitudes. This could explain the hummocky texture of the bright plains of the Chaac-Camaxtli region. However, Figure 4 indicates that the surroundings of Chaac deviate somewhat from this scheme. Indeed in this region the SO₂ abundance rises substantially to a level of 50–55% and sometimes higher whereas the grain sizes remain coarse. Such values might be the sign of an increased stability for SO₂ frost near Chaac Patera.

[33] In the Chaac-Camaxtli region, the white unit within Balder Patera has the highest concentration of SO₂ (>90% SO₂ assuming intimate mixing [*Lopes et al.*, 2001]), and could be an SO₂ flow [*Smythe et al.*, 2000]. The southern part of the Chaac-Camaxtli region is relatively rich in SO₂ compared to the rest of the region, which is probably due to SO₂ deposition from the Prometheus plume(s). There is no clear correlation of visible color and SO₂ content in the bright plains. The composition of the uppermost plains material is complex; *Fanale et al.* [1974] suggested that the white-colored bright plains may represent a coating of some sulfur-bearing compound other than SO₂, perhaps anhydrous salts. *Lopes-Gautier et al.* [2000] suggested that the visible bright ring at Prometheus, which does not correspond to a ring of SO₂-enrichment as detected by NIMS, may indicate the presence of other compounds on the plains. Io's plumes appear to eject gases of more than one composition; *Spencer et al.* [2000] detected the presence of both S₂ and SO₂ in a single plume at Pele.

[34] One important insight regarding the bright plains has come from our mapping. We note that within the outer scarps of Chaac, Grannos, Ababinili, and Steropes Paterae, there are regions that have the same basic color as the bright plains material but lack the well developed texture seen in the bright plains away from the paterae. We have mapped these regions as bright plains material (p_b) rather than as patera floor material (pf_b or pf_a). We think it possible that these regions were originally dark patera floor material, but as activity waned in these parts of the paterae, sulfur-bearing materials were able to accumulate over time, thus transforming these regions into bright plains. This process may be at an early to intermediate stage in Chaac and Ababinili Patera, in an advanced stage in Grannos and Steropes Paterae, and in a very advanced stage in the irregular feature in the upper right of the map area. If the dark patera floor material is dominantly mafic to ultramafic silicate in composition, and if at least part of Io's bright plains are formed by this process, then this process might explain how Io's crust can support some of the tall mountains seen in Voyager and Galileo images. *Clow and Carr* [1980] and *Carr et al.* [1998] suggested that if Io's crust was dominated by sulfur, then it would not have the strength to support steep caldera walls and tall mountains. If Io's crust

is dominantly mafic or ultramafic silicate and only covered in its uppermost layers with various sulfur-bearing compounds, then the crust should have the strength to support these features.

5.4. Age Relationships

[35] The map units have been described in part on the assumption that color differences represent compositional differences. It appears, if this is true, that all volcanic eruption styles are continuing to occur, and that all lava compositions are continuing to be emplaced. It is possible, however, that some of the map units represent varying stages in the time evolution of surface materials. The dark units, such as pf_d and f_d , are also the sources of most of the heat output observed by NIMS, and they must therefore be the most recently emplaced. A subset of the pf_d unit is that of slightly greenish, or less dark, patera floor material that is slightly older and cooler material. It was noted, for example, that the floor of Chaac appeared to have lightened slightly since Voyager. The bright patera floor material (pf_b) is remarkably solid and continuous in many paterae, similar to the dark (pf_d) material, but much lighter in color. Perhaps these regions are older silicate flows that have cooled sufficiently such that coatings of SO_2 frosts or thin sulfur flows accumulate on upper surfaces and do not sublimate away, causing color or albedo variations. Thus in the Chaac-Camaxtli region a potential age progression can be observed among its features, based mainly on color and assumed temperature. However, it is important to note that we cannot demonstrate that a darker unit in one patera is not older than a less dark unit in another patera. Also, there appear to be textural and brightness differences in the background bright plains not directly attributable to pyroclastic mantling. This observation may imply some variation in the composition of the plains, or in the process(es) that form or degrade them.

5.5. Topographic Relationships

[36] There appears to be a weak relationship between volcanic activity and topography. Sobo Fluctus, which occurs in a topographic low, has produced the widest variety of volcanic deposits (bright flows, dark flows, dark pyroclastics, bright pyroclastics, red pyroclastics) which cover the largest part of the map area in a roughly northwest-southeast linear trend. Material in Sobo erupts from several point sources, which we speculate may mark the locations of magma conduits in a well fractured crust. Flows clearly spill out and partially fill a broad topographic depression. In contrast, flows in paterae are confined by the steep walls of calderas. Other active hot spots in NIMS data (Utu, Tien Mu) also occur in topographic lows. In contrast, the least active centers (Chaac, Balder, Grannos, and possibly Ababinili) occur on topographic highs. Camaxtli and Mentu, which might be called 'intermediately' active (compared to the others mentioned above), occur in a topographic transition (from low to high). Ruaumoko (very active) and Steropes (inactive) do not follow the pattern.

5.6. Subsurface Relationships

[37] From mapping of the Chaac-Camaxtli region, we can make the following observations: 1) volcanic vents within paterae have migrated (on the scale of tens of kilometers) with time, at least over the last 21 years; and 2) most of the

active centers are associated with relative topographic lows, and that paterae on topographic highs tend to be less active. What subsurface relationships might explain this activity?

[38] If we assume that the visible deposits are related to the underlying magma chamber volumes, then we can make some comments for the specific centers, but only in terms of the most recent activity. Volumetrically, the largest amount of recent volcanic material has been emplaced in Sobo Fluctus, which the NIMS data shows was the brightest hot spot in our map region during I24 and I27 [Lopes *et al.*, 2001]. The areal coverage of the darkest Sobo flows is ~ 115 sq. km. It must have the largest magma source region, to supply material for several vents separated by ~ 75 km. Ruaumoko Patera, with its dark floor covering ~ 31 sq. km, was the second brightest in I24, whereas the irregular Utu Patera was the second brightest in I27 [Lopes *et al.*, 2001]. It has a dark floor at its northern end covering ~ 28 sq. km. Ruaumoko appears to fall topographically above Sobo, and Utu may occur in a topographic low. Although we don't know the thickness of materials in these paterae, by areal extent alone it is clear that Sobo has emplaced much more material than the next two brightest hot spots. Chaac, though much larger, has recently only emplaced a small amount of fresh dark material at its extreme southern end (~ 5 sq. km). It falls in an apparent topographic high. Camaxtli is still an active hot spot, but the areal extent of its darkest flows is less than the darkest flows at Sobo (~ 50 sq. km). It appears to occur topographically above Sobo.

[39] The simplest explanation is that active volcanism in this region is being influenced by crustal thickness: where the crust is thicker (topographic highs), dense mafic to ultramafic melts have a harder time erupting onto the patera floors, and produce flows of limited areal extent (and presumably volume). In contrast, where the crust is thinner (topographic lows), dense magmas erupt onto the surface, producing areally extensive dark flows and (presumably) extensive secondary bright flows of remobilized crustal sulfur-bearing material. This is analogous to the distribution of high-titanium mare lavas on the Earth's moon: extensive dense high-titanium lava flows filled large nearside basins where the crust was thinned (in the Moon's case) by impact cratering, whereas on the lunar farside (where the crust is thicker) lavas are restricted to a few crater interiors, and dense high-titanium lavas are rare or absent [e.g., *Wilhelms*, 1987; *Robinson et al.*, 1992; *Greeley et al.*, 1993; *Williams et al.*, 1995]. In the case of the Chaac-Camaxtli region of Io, crustal thickness variations are not due to impacts, but some other process(es), perhaps related to tidal activity.

[40] In any case, the crust is exerting some control on magma access to the surface. The linear trend of the paterae and the irregular shapes of many of the patera margins suggest that fractures caused by tectonic activity may influence magma movement, and may be responsible for the vent migration. The spacing of the volcanic vents in this region is mostly uniform, on the order of 100–150 km. In addition, the paterae and vents seem to lie along two trends, one at 45 degrees and one at 135 degrees from north, and the straight edges on some paterae follow these same trends. These observations suggest a pattern of subsurface crustal fracturing. Most of the paterae in this region have irregular margins, having one or more straight sides or sharp corners. This indicates tectonic forces may influence the formation

and/or evolution of some of the paterae [Jaeger *et al.*, 2001]. A shadow measurement revealed that the walls of Chaac Patera are 2.7 km deep with a 70 degree slope. This indicates that a tremendous amount of vertical movement occurred in the crust, and also indicates that the crust is made of materials capable of supporting extremely steep slopes without mass wasting [Radebaugh *et al.*, 2001].

[41] The active tectonism in this region may influence the ability of magma to reach the surface. Because of the variability of tidal stresses within Io's lithosphere, it is possible that some regions experience extension, followed by compression. During the times of extension, magma can exploit the fractures in the lithosphere and thus reach the surface to erupt. When there is compression, these pathways are sealed off to magma access. If Io's lithosphere is underlain by a global, partially crystalline, magma ocean [Keszthelyi *et al.*, 1999], then volcanic activity in all parts of our map area is equally likely, so that eruption locations are more likely controlled by the ability of magma to ascend to the surface. Thus the changes in vent locations could have more to do with local tectonic changes.

5.7. Implications for Io

[42] With the notable exception of Io's tall mountains, this region contains most of the major surface features found elsewhere on Io. The effusive, multihued eruptions seen in this region are similar to those seen at Culann Patera, some 30 degrees south of Chaac [McEwen *et al.*, 2000]. The presence of hot spots detected by NIMS shows that this region is currently active [Lopes *et al.*, 2001]. The color range and extents of the diffuse deposits in this region suggest that volatile-rich eruptions are an important component in Io's volcanic activity.

[43] Io is covered in paterae, nearly 300 of which contain materials similar to the dark patera floor material unit (pf_d), indicating geologically recent activity [Radebaugh *et al.*, 2001]. This region is one with exceptionally high numbers of paterae per a unit area; a study of paterae on Io revealed that the number density of paterae is higher at equatorial regions and at longitudes of about 330°W and 150°W longitude [Radebaugh *et al.*, 2001]. In addition, paterae in these regions are smaller and more continuously active than the global average. Schenk *et al.* [2001] suggest that there is an anticorrelation between these regions of high patera density and the presence of mountains. None of the eleven paterae in the Chaac-Camaxtli region (and none of the 15 or so paterae in regions surrounding our study area) is adjacent to a mountain or plateau, in comparison with the global figure of 13% of 417 paterae on Io that are adjacent to mountains [Radebaugh *et al.*, 2001]. In addition, none of the paterae appear to have formed as pull-apart basins, such as at Hi'iaka Patera [Jaeger *et al.*, 2001]. It will be interesting to compare our mapping results from this region of Io's anti-Jovian hemisphere with another which contains a mountain and paterae in close proximity (e.g., Tohil Mons/Paterae) to assess these volcano-tectonic relationships further. This is planned as future work.

[44] Formation of paterae can occur through one of the six following models [Radebaugh *et al.*, 2001]: 1) Flank eruptions leading to patera formation atop shields through collapse of overlying material into an evacuated magma chamber. No evidence exists in the Chaac-Camaxtli region

for flank eruptions; 2) Piston-like collapse over an evacuated shallow magma chamber resulting in formation of a patera, the dimensions of which are similar to the magma chamber volume before eruption; 3) Dikes of mafic magma that rise through the crust and then make contact with frozen volatiles in the crust, leading to an explosive plume eruption of SO₂ frost and subsequent collapse of the evacuated subsurface; 4) Some paterae may form in concert with the formation or evolution of mountains, since morphologies of patera margins are irregular near mountains. There are, however, no mountains in this mapped region; 5) Some paterae may form as graben-type features, by the pulling apart of crustal material. Extensional features of this nature are not observed in this area; 6) Dense magma or solidified intrusive material that has accumulated in the crust can sink back down into the mantle, creating a void over which overlying crustal material collapses. It is possible this has happened at some paterae in the Chaac-Camaxtli region, although the magma systems had to have been reactivated, allowing fresh magma to flow onto the floors of the paterae.

[45] From our study of the paterae in the Chaac-Camaxtli region, we can determine that of these six models for patera formation, the only two that can be considered here are those of foundering of a patera floor over a shallow magma reservoir, or disintegration of a patera floor due to volatilization of crustal materials from interaction with mafic magma. In both of these scenarios, there is a loss of crustal material, either to collapse or to volatilization, and there is apparently not an equal replacement of this crustal material with lava flows. This loss of material is inextricably tied to the style of volcanism for the region, and as yet it is not completely understood.

6. Conclusions

[46] Using high-, medium-, and low-resolution SSI images from recent Galileo flybys (1999–2000) [Keszthelyi *et al.*, 2001], along with NIMS spectral data processed for temperature estimates and compositional information [Douté *et al.*, 2001; Lopes *et al.*, 2001], we have produced a geologic/geomorphologic map of the Chaac-Camaxtli region of Io's leading anti-Jovian hemisphere. This is the first regional map of Io made from Galileo data. Our mapping shows that the Chaac-Camaxtli region is dominated by 11 volcanic centers, several of which are active hot spots [Lopes *et al.*, 2001]. Most of these centers are paterae analogous in morphology to terrestrial calderas, although there are differences in size and shape. We have identified 9 mappable units in this region, which are interpreted to represent a range of lava compositions and eruption styles that were emplaced in the recent geologic past. Interactions between silicate lavas and volatile, sulfur-bearing compounds appear to be very important in producing Io's diverse volcanic products. Mapping of structural features show that most of the active regions are associated with distinct topographic lows, and most paterae show a relatively regular spacing (~100–150 km), suggesting that Io's lithosphere may be well-fractured to accommodate rising magma. This may explain the migration of dark hot spots regions within paterae in the 21 years between Voyager and Galileo observations on this region. Dark patera floors may evolve over time into bright plains, which if composed of mafic to

ultramafic compositions (as inferred from analysis of NIMS hot spot [Lopes-Gautier et al., 1999; Lopes et al., 2001] and SSI spectral data [Geissler et al., 1999]), may explain the strength of Io's crust to support steep patera walls and tall mountains [Clow and Carr, 1980; Carr et al., 1998].

[47] We propose using the mapping units and approach developed in this paper as a guide to further geologic mapping using Galileo images of Io. We plan to map other areas of Io (e.g., Culann-Tohil) using integrated Galileo SSI/NIMS data to better understand the geologic evolution of these areas. An excellent set of SSI observations was obtained of this region during the Galileo I32 Io flyby (October, 2001), which will aid our ever-evolving understanding of this volcanic moon.

[48] **Acknowledgments.** We would like to acknowledge Jason Perry and Jennifer Blue, for choosing the names for the newly identified paterae in our map region. This research was supported by the National Aeronautics and Space Administration under the Jovian System Data Analysis Program (JSDAP) Grant NAG5-8897. The authors would also like to thank Paul Lucey and an anonymous individual for very helpful reviews.

References

- Bender, K. C., J. W. Rice Jr., D. E. Wilhelms, and R. Greeley, Geologic map of Callisto, *U.S. Geol. Surv. Misc. Invest. Ser., Map I-2581*, 1:15,000,000, 1997.
- Boyce, J. M., Ages of flow units in the lunar nearside maria based on Lunar Orbiter IV photographs, *Proc. Lunar Sci. Conf., 7th*, 2717–2728, 1976.
- Carlson, R. W., et al., The distribution of sulfur dioxide and other infrared absorbers on the surface of Io, *Geophys. Res. Lett.*, *24*, 2479–2482, 1997.
- Carr, M. H., K. A. Howard, and F. El-Baz, Geologic maps of the Apennine-Hadley region of the Moon, *U.S. Geol. Surv. Misc. Invest. Ser., Map I-723*, 1:250,000, 1971.
- Carr, M. H., A. S. McEwen, K. A. Howard, F. C. Chuang, P. Thomas, P. Schuster, J. Oberst, G. Neukum, and G. Schubert, Mountains and calderas on Io: Possible implications for lithosphere structure and magma generation, *Icarus*, *135*, 146–165, 1998.
- Clow, G. D., and M. H. Carr, Stability of sulfur slopes on Io, *Icarus*, *44*, 268–279, 1980.
- Collins, G. C., J. W. Head, and R. T. Pappalardo, The role of extensional instability in creating Ganymede grooved terrain: Insights from Galileo high-resolution stereo imaging, *Geophys. Res. Lett.*, *25*, 233–236, 1997.
- Crown, D. A., R. Greeley, R. A. Craddock, and G. G. Schaber, Geologic map of Io, *U.S. Geol. Surv. Misc. Invest. Ser., Map I-2209*, 1:15,000,000, 1992.
- Davies, A. G., L. P. Keszthelyi, D. A. Williams, C. B. Phillips, A. S. McEwen, R. M. Lopes-Gautier, W. D. Smythe, L. A. Soderblom, and R. W. Carlson, Thermal signature, eruption style, and eruption evolution at Pele and Pillan on Io, *J. Geophys. Res.*, *106*, 33,079–33,103, 2001.
- Douté, S., B. Schmitt, R. Lopes-Gautier, R. Carlson, L. Soderblom, and J. Shirley, Mapping SO₂ frost on Io by the modeling of NIMS hyperspectral images, *Icarus*, *149*, 107–132, 2001.
- Douté, S., R. Lopes, L. W. Kamp, R. Carlson, and B. Schmidt, Dynamics and evolution of SO₂ gas condensation around Prometheus-like volcanic plumes on Io as seen by the Near Infrared Mapping Spectrometer, *Icarus*, in press, 2002.
- Fanale, F. P., T. V. Johnson, and D. L. Matson, Io: A surface evaporite deposit?, *Science*, *186*, 922–925, 1974.
- Fink, J. H., S. O. Park, and R. Greeley, Cooling and deformation of sulfur flows, *Icarus*, *56*, 38–50, 1983.
- Geissler, P. E., A. S. McEwen, L. Keszthelyi, R. Lopes-Gautier, J. Granahan, and D. P. Simonelli, Global color variations on Io, *Icarus*, *140*, 265–282, 1999.
- Greeley, R., and J. E. Guest, Geologic map of the eastern equatorial region of Mars, *U.S. Geol. Surv. Misc. Invest. Ser., Map I-1802-B*, 1:15,000,000, 1987.
- Greeley, R., E. Theilig, and P. Christensen, The Mauna Loa sulfur flow as an analog to secondary sulfur flows (?) on Io, *Icarus*, *60*, 189–199, 1984.
- Greeley, R., P. D. Spudis, and J. E. Guest, Geologic map of the Ra Patera area of Io, *U.S. Geol. Surv. Misc. Invest. Ser., Map I-1949*, 1:2,000,000, 1988.
- Greeley, R., et al., Galileo imaging observations of lunar maria and related deposits, *J. Geophys. Res.*, *98*, 17,183–17,206, 1993.
- Hapke, B., The surface of Io: A new model, *Icarus*, *79*, 56–74, 1989.
- Hapke, B., and F. Graham, Spectral properties of condensed phases of disulfur monoxide, polysulfur oxide, and irradiated sulfur, *Icarus*, *79*, 47–55, 1989.
- Kargel, J. S., P. Delmelle, and D. B. Nash, Volcanogenic sulfur on Earth and Io: Composition and spectroscopy, *Icarus*, *142*, 249–280, 1999.
- Keszthelyi, L., A. S. McEwen, and G. J. Taylor, Revisiting the hypothesis of a mushy global magma ocean in Io, *Icarus*, *141*, 415–419, 1999.
- Keszthelyi, L. P., A. S. McEwen, C. B. Phillips, M. Milazzo, P. E. Geissler, D. A. Williams, E. Turtle, J. Radebaugh, and D. Simonelli, Imaging of volcanic activity on Jupiter's moon Io by Galileo during GEM and GMM, *J. Geophys. Res.*, *106*, 33,025–33,052, 2001.
- Kieffer, S. W., R. Lopes-Gautier, A. McEwen, W. Smythe, L. Keszthelyi, and R. Carlson, Prometheus: Io's wandering plume, *Science*, *288*, 1204–1208, 2000.
- Jaeger, W., E. P. Turtle, L. P. Keszthelyi, and A. S. McEwen, Orogenic tectonism on Io, *Proc. Lunar Planet. Sci. Conf. 32nd*, abstract 2045, 2001.
- Johnson, R. E., Polar "caps" on Ganymede and Io revisited, *Icarus*, *128*, 448–469, 1997.
- Johnson, J. R., G. Komatsu, and V. R. Baker, Geologic map of the Barrymore Quadrangle (V-59), Venus, *U.S. Geol. Surv. Geol. Invest. Ser., Map I-2610*, 1:5,000,000, 1999.
- Lopes-Gautier, R., et al., Active volcanism on Io: Global distribution and variations in activity, *Icarus*, *140*, 243–264, 1999.
- Lopes-Gautier, R., et al., A close-up look at Io from Galileo's Near-Infrared Mapping Spectrometer, *Science*, *288*, 1201–1204, 2000.
- Lopes, R. M. C., et al., Io in the near infrared: NIMS results from the Galileo fly-bys in 1999 and 2000, *J. Geophys. Res.*, *106*, 33,053–33,078, 2001.
- Lucchitta, B. K., Geologic map of Ophir and Central Candor Chasmata (MTM-05072) of Mars, *U.S. Geol. Surv. Misc. Invest. Ser., Map I-2568*, 1:500,000, 1999.
- McEwen, A. S., et al., High-temperature silicate volcanism on Jupiter's moon Io, *Science*, *281*, 87–90, 1998a.
- McEwen, A. S., et al., Active volcanism on Io as seen by Galileo SSI, *Icarus*, *135*, 181–219, 1998b.
- McEwen, A. S., et al., Galileo at Io: Results from high-resolution imaging, *Science*, *288*, 1193–1198, 2000.
- McGill, G. E., Geologic map of the Sappho Patera Quadrangle (V-20), Venus, *U.S. Geol. Surv. Geol. Invest. Ser., Map I-2637*, 1:5,000,000, 2000.
- Milazzo, M. P., L. P. Keszthelyi, and A. S. McEwen, Observations and initial modeling of lava-SO₂ interactions at Prometheus, Io, *J. Geophys. Res.*, *106*, 33,121–33,128, 2001.
- Moore, H. J., Geologic map of the Maasaw Patera area of Io, *U.S. Geol. Surv. Misc. Invest. Ser., Map I-1851*, 1:1,003,000, 1987.
- Moore, J. M., R. J. Sullivan, R. T. Pappalardo, E. P. Turtle, and the Galileo SSI Team, Degradation and deformation of scarps and slopes on Io: New results, *Lunar Planet. Sci. [CD-ROM]*, XXXI, abstract 1531, 2000.
- Moore, J. M., R. J. Sullivan, F. C. Chuang, J. W. Head III, A. S. McEwen, M. P. Milazzo, B. E. Nixon, R. T. Pappalardo, P. M. Schenk, and E. P. Turtle, Landform degradation and slope processes on Io: The Galileo view, *J. Geophys. Res.*, *106*, 33,223–33,240, 2001.
- Murase, T., and A. R. McBirney, Properties of some common igneous rocks and their melts at high temperatures, *Geol. Soc. Am. Bull.*, *84*, 3563–3592, 1973.
- Nash, D. B., and F. P. Fanale, Io's surface composition based on reflectance spectra of sulfur/salt mixtures and proton-irradiation experiments, *Icarus*, *31*, 40–80, 1977.
- Nash, D. B., M. H. Carr, J. Gradie, D. M. Hunten, and C. F. Yoder, Io, in *Satellites*, edited by J. A. Burns and M. S. Matthews, pp. 629–688, Univ. of Ariz. Press, Tucson, 1986.
- Nelson, R. M., and B. W. Hapke, Spectral reflectivities of the Galilean satellites and Titan, 0.32 to 0.86 micrometers, *Icarus*, *36*, 304–329, 1978.
- Nelson, R. M., W. D. Smythe, B. W. Hapke, and A. J. Cohen, On the effect of X-rays on the color of elemental sulfur: Implications for Jupiter's satellite Io, *Icarus*, *85*, 326–334, 1990.
- Neukum, G., and B. A. Ivanov, Crater size distributions and impact probabilities of Earth from lunar, terrestrial-planet, and asteroid cratering data, in *Hazards Due to Comets and Asteroids*, edited by T. Gehrels, pp. 359–416, Univ. of Ariz. Press, Tucson, 1994.
- Pieri, D. C., S. M. Baloga, R. M. Nelson, and C. Sagan, Sulfur flows of Ra Patera, Io, *Icarus*, *60*, 685–700, 1984.
- Phillips, C. B., Voyager and Galileo views of volcanic resurfacing on Io and the search for geologic activity on Europa, Ph.D. dissertation, 269 pp., Univ. of Ariz., Tucson, 2000.

- Radebaugh, J., L. P. Keszthelyi, A. S. McEwen, E. P. Turtle, W. Jaeger, and M. Milazzo, Paterae on Io: A new type of volcanic caldera?, *J. Geophys. Res.*, *106*, 33,005–33,020, 2001.
- Robinson, M. R., B. R. Hawke, P. G. Lucey, and G. A. Smith, Mariner 10 multispectral images of eastern limb and farside of the Moon, *J. Geophys. Res.*, *97*, 18,265–18,274, 1992.
- Sagan, C., Sulphur flows on Io, *Nature*, *280*, 750–753, 1979.
- Schaber, G. G., D. H. Scott, and R. Greeley, Geologic map of the Ruwa Patera quadrangle (Ji-2) of Io, *U.S. Geol. Surv. Geol. Invest. Ser., Map I-1980*, 1:5,000,000, 1989.
- Schenk, P. M., and W. B. McKinnon, Fault offsets and lateral crustal movement on Europa: Evidence for a mobile ice shell, *Icarus*, *79*, 75–100, 1989.
- Schenk, P., H. Hargitai, R. Wilson, A. McEwen, and P. Thomas, The mountains of Io: Global and geological perspectives from Voyager and Galileo, *J. Geophys. Res.*, *106*, 33,201–33,222, 2001.
- Scott, D. H., and M. H. Carr, Geologic map of Mars, *U.S. Geol. Surv. Misc. Invest. Ser., Map I-1083*, 1:25,000,000, 1978.
- Shoemaker, E. M., and R. J. Hackman, Stratigraphic basis for a lunar time scale, in *The Moon*, edited by Z. Kopal and Z. K. Mikhailov, pp. 289–300, Academic, San Diego, Calif., 1962.
- Smith, B. A., et al., The Jupiter system through the eyes of Voyager 1, *Science*, *204*, 951–972, 1979a.
- Smith, B. A., et al., The Galilean satellites and Jupiter: Voyager 2 imaging science results, *Science*, *206*, 927–950, 1979b.
- Smythe, W. D., R. Lopes-Gautier, S. Douté, S. W. Kieffer, R. W. Carlson, L. Kamp, and F. E. Leader, Evidence for massive sulfur dioxide deposit on Io, *Bull. Am. Astron. Soc.*, *32*(3), 1047, 2000.
- Spencer, J. R., A. S. McEwen, M. A. McGrath, P. Sartoretti, D. B. Nash, K. S. Noll, and D. Gilmore, Volcanic resurfacing of Io: Post-repair HST imaging, *Icarus*, *127*, 221–237, 1997.
- Spencer, J. R., K. L. Jessup, M. A. McGrath, G. E. Ballester, and R. Yelle, Discovery of gaseous S₂ in Io's Pele plume, *Science*, *288*, 1208–1210, 2000.
- Studel, R., G. Holdt, and A. T. Young, On the colors of Jupiter's satellite Io: Irradiation of solid sulfur at 77 K, *J. Geophys. Res.*, *91*, 4971–4977, 1986.
- Tanaka, K. L., et al., *The Venus Geologic Mappers Handbook*, *U.S. Geol. Surv. Open File Rep.*, 94–438, 66 pp., 1994.
- Wagner, R. J., R. Jaumann, and G. P. Neukum, Geologic map of the Etana region (Jg-1) of Ganymede, *U.S. Geol. Surv. Misc. Invest. Ser., Map I-2497*, 1:5,000,000, 1995.
- Whitford-Stark, J. L., P. J. Mouginiis-Mark, and J. W. Head, Geologic map of the Lerna region (Ji-4) of Io, *U.S. Geol. Surv. Misc. Invest. Ser., Map I-2055*, 1:5,000,000, 1991.
- Wilhelms, D. E., Geologic mapping of the second planet, in *Astrogeology*, vol. 55, *U.S. Geol. Surv. Interagency Rep.*, 36 pp., 1972.
- Wilhelms, D. E., The geologic history of the Moon, *U.S. Geol. Surv. Prof. Pap.*, *1348*, 302 pp., 1987.
- Wilhelms, D. E., Geologic mapping, in *Planetary Mapping*, edited by R. Greeley and R. M. Batson, pp. 208–260, Cambridge Univ. Press., New York, 1990.
- Wilhelms, D. E., and J. F. McCauley, Geologic map of the near side of the Moon, *U.S. Geol. Surv. Misc. Invest. Ser., Map I-703*, 1:5000000, 1971.
- Williams, D. A., R. Greeley, G. Neukum, R. Wagner, and S. D. Kadel, Multispectral studies of western limb and farside maria from Galileo Earth-Moon Encounter 1, *J. Geophys. Res.*, *100*, 23,291–23,299, 1995.
- Williams, D. A., A. H. Wilson, and R. Greeley, A komatiite analog to potential ultramafic materials on Io, *J. Geophys. Res.*, *105*, 1671–1684, 2000.
- Williams, D. A., A. G. Davies, L. P. Keszthelyi, and R. Greeley, The July 1997 eruption at Pillan Patera on Io: Implications for ultrabasic lava flow emplacement, *J. Geophys. Res.*, *106*, 33,105–33,119, 2001a.
- Williams, D. A., R. Greeley, R. M. C. Lopes, and A. G. Davies, Evaluation of sulfur flow emplacement on Io from Galileo Data and numerical modeling, *J. Geophys. Res.*, *106*, 33,161–33,174, 2001b.
- Wong, M. C., and R. E. Johnson, The effect of plasma heating on sublimation-driven flow in Io's atmosphere, *Icarus*, *115*, 109–118, 1995.
- Young, A. T., No sulfur flows on Io, *Icarus*, *58*, 197–226, 1984.
- Zahnle, K., L. Dones, and H. F. Levison, Cratering rates on the Galilean satellites, *Icarus*, *136*, 202–222, 1999.

S. Douté and R. M. C. Lopes, NASA Jet Propulsion Laboratory, 4800 Oak Grove Drive, Mail Stop 183-601, Pasadena, CA 91109, USA.

R. Greeley and D. A. Williams, Department of Geological Sciences, Arizona State University, Box 871404, Tempe, AZ 85287, USA. (williams@dione.la.asu.edu)

L. P. Keszthelyi, A. S. McEwen, and J. Radebaugh, Lunar and Planetary Laboratory, University of Arizona, Tucson, AZ 85721, USA.